DISCLAIMER NOTICE

THIS DOCUMENT IS BEST QUALITY PRACTICABLE. THE COPY FURNISHED TO DTIC CONTAINED A SIGNIFICANT NUMBER OF PAGES WHICH DO NOT REPRODUCE LEGIBLY.

Report 1759

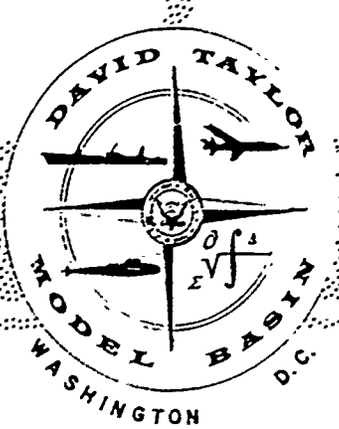

DEPARTMENT OF THE NAVY

HYDROMECHANICS

AERODYNAMICS

STRUCTURAL MECHANICS

APPLIED MATHEMATICS

THE ELASTIC BUCKLING STRENGTH OF SPHERICAL GLASS SHELLS

by

Martin A. Krenzke

and

Robert M. Charles

STRUCTURAL MECHANICS LABORATORY

RESEARCH AND DEVELOPMENT REPORT

September 1963 Report 1759

THE ELASTIC BUCKLING STRENGTH OF SPHERICAL GLASS SHELLS

by

Martin A. Krenzke

and

Robert M. Charles

September 1963

Report 1759
S-R011 01 01

TABLE OF CONTENTS

	Page
ABSTRACT	1
INTRODUCTION	1
BACKGROUND ON RECENT MODEL BASIN TESTS OF MACHINED SPHERICAL SHELLS	2
DESCRIPTION OF MODELS	4
TEST PROCEDURE AND RESULTS	5
DISCUSSION	6
SUMMARY	8
RECOMMENDATIONS	8
ACKNOWLEDGMENT	9
REFERENCES	21

LIST OF FIGURES

Figure 1 – Effect of Initial Imperfections on the Elastic Buckling Coefficient for Spherical Shells	10
Figure 2 – Notation Used for the Imperfect Shell	10
Figure 3 – Model during Inspection	11
Figure 4 – Model before and after Test	12
Figure 5 – Comparison of Experimental Collapse Pressure with Empirical Design Equation for Initially Imperfect Spheres	13
Figure 6 – Experimental Collapse Depth versus Ratio of Weight to Displacement	14
Figure 7 – Estimated Collapse Depth versus Ratio of Weight to Displacement for Near-Perfect Spheres	16

LIST OF TABLES

Page

Table 1 – Measured Shell Thicknesses, Hand-Blown Series 17

Table 2 – Measured Shell Thicknesses, Ground and Polished Series 18

Table 3 – Measured Model Dimensions 19

Table 4 – Experimental Collapse Pressures 20

Table 5 – Critical Imperfection Geometry 20

ABSTRACT

The potential of spherical glass shells for deep-submergence applications was explored by determining the hydrostatic-collapse strength of 20 hemispheres of annealed Pyrex glass. The experimental collapse pressures, which ranged between 6700 and 43,250 psi, were adequately calculated using an empirical design equation for the elastic buckling strength of initially imperfect spheres. Maximum stress levels of about 300,000 psi were obtained in these tests. These results do not demonstrate the maximum compressive strength of Pyrex glass since each failure initiated in the elastic buckle range. The tests verify earlier calculations which indicated that spheres of Pyrex glass or of other "bridgmanite" materials have an outstanding strength-to-weight advantage over any other type hull using known materials. However, the long-term mechanical properties of glass in a marine-environment must be evaluated before its potential for deep-submergence applications may be properly assessed.

INTRODUCTION

Glass has a rather poor reputation as a structural material. It is generally accepted that annealed, unstrengthened glass (glass without an initial compressive stress near its surfaces) is susceptible to catastrophic failure initiating in its surface when under relatively low tensile loads. Recent advances in the chemical strengthening of glass, however, greatly increase its ability to resist tension loads and make it appear very attractive for many structural applications.

Until recently, the extremely high compressive strength of glass, both in the annealed and in the surface compressed condition, was a somewhat lesser known property. Little attention has been drawn to tests conducted by Bridgman,[1] which demonstrated the unbelievable resistance which glass offers to compressive loads. By subjecting thick-walled glass* cylinders with about a 3 to 1 ratio of external to internal radius to pressures of 400,000 psi, Bridgman obtained calculated compressive stress levels of 800,000 psi without fracture.

Unaware of Bridgman's earlier work, and in search of new materials for deep-submergence applications, the David Taylor Model Basin conducted exploratory hydrostatic tests of 20 long, unstiffened cylinders of No. 7740 glass.[2] The results of this study indicated that glass, with its high compressive strength and relatively low weight, has considerable potential as a material for deep-depth hulls. Specifically, calculations based on these test

---

[1] References are listed on page 21.

*The full details of these early experiments have been lost. However, it is probable that the glass was a soda-lime glass since Pyrex was not available at that time.

results and those of near-perfect aluminum hemispheres[3,4] indicated that glass spheres have a potential of demonstrating far higher strength-to-weight ratios than attainable by any other type hull using currently available materials.

To positively demonstrate the performance of spherical glass shells, 20 glass hemispheres were tested to collapse under external hydrostatic pressure. This report summarizes these test results, compares the experimental collapse pressures with pressures calculated using an empirical equation for near-perfect spherical shells, and compares the strength-weight characteristics of glass spheres with those of spheres of other materials.

BACKGROUND ON RECENT MODEL BASIN TESTS OF MACHINED SPHERICAL SHELLS

The classical small-deflection theory for the elastic buckling of a complete sphere was first developed by Zoelly in 1915 and has been summarized by Timoshenko.[5] In this analysis it is assumed that buckling will occur at that pressure which permits an equilibrium shape which is minutely removed from the perfectly spherical deflected shape. The general expression for this classical buckling pressure p_{cr} may be given as

$$p_{cr} = \frac{K E (h/R)^2}{\sqrt{1 - \nu^2}} \qquad [1]$$

where K is a buckling coefficient,
E is Young's modulus,
h is the shell thickness,
R is the radius to the midsurface of the shell, and
ν is Poisson's ratio.

A small-deflection buckling coefficient K_1 of 1.15 was obtained by Zoelly for initially perfect spheres. Thus, his classical small-deflection, linear buckling theory for initially perfect spheres may be expressed as

$$p_1 = \frac{1.15 E (h/R)^2}{\sqrt{1 - \nu^2}} \qquad [2]$$

Unfortunately, the very limited data existing prior to recent Model Basin tests do not support the linear theory; elastic buckling coefficients of roughly one-fourth the classical value were observed in earlier tests recorded in the literature.[6] Various investigators have attempted to explain this discrepancy by introducing nonlinear, large-deflection shell equations. In effect, their expressions for the theoretical buckling pressures resulting from the nonlinear equations take the same general form as Equation [1]. However, the elastic buckling coefficients are often about one-fourth of the classical coefficient K_1 and thus are generally in

fair agreement with the early experiments. A more complete background on these large deflection analyses is given in References 6 and 7.

The test specimens used in the earlier tests, the results of which have been frequently compared to the theoretical buckling pressures for initially perfect spheres, were formed from flat plates. Thus, although little data are available, it can be assumed that these early specimens had significant departure from sphericity as well as variations in thickness and residual stresses. Those specimens which were not complete spheres also had adverse boundary conditions. Since initial imperfections affect collapse strength, the comparison of existing theory, both linear and nonlinear, with the early experiments is not valid. Until very recently, however, no attempt has been made to theoretically evaluate the effect of initial imperfections on the collapse strength of deep or complete spheres.

To clarify this rather large discrepancy between the classical buckling pressure and the early experimental data recorded in the literature, the Model Basin has launched a rather extensive experimental program.* Test specimens are being machined as well as manufactured according to feasible large-scale fabrication procedures. To date, however, most of the results have been obtained from small machined models. Although this program is at a relatively early stage, advances have been made in understanding the collapse mechanism and in the rational design of spherical shells.

Three series of models have been machined to study the experimental collapse strength of near-perfect deep spherical shells.[3,4,7] Ratios of experimental collapse pressure to the pressure obtained from classical small-deflection theory of about 0.7 to 0.9 were obtained. These ratios are considerably higher than the ratios obtained in previous tests recorded in the literature, and they demonstrate the detrimental effects of initial imperfections on collapse strength. Since these models had small, unavoidable imperfections, the experimental results lend considerable support to the validity of the small-deflection analysis for the elastic buckling strength of initially perfect spheres.

The effect of initial imperfections or unevenness factors on the elastic buckling coefficients obtained in recent Model Basin tests of deep spherical shells is discussed in Reference 4 and shown graphically in Figure 1. It is illustrated in Figure 1 that no single buckling coefficient may be used in Equation [1] to calculate the strength of spherical shells which have varying degrees of initial imperfections. However, it is also illustrated in Figure 1 that although the classical buckling coefficient is apparently valid for perfect spheres, it is impossible to manufacture or measure most spherical shells with sufficient perfection to justify the use of the classical equation in design.

Based on the results presented in Figure 1, the Model Basin has recommended the following empirical equation for the elastic buckling strength of near-perfect spheres.[3,4,7]

*This program covers both the elastic and inelastic strength of spherical shells. Since this present study is concerned with elastic strength only, a discussion of inelastic strength is omitted.

$$P_3 = \frac{0.8\,E\,(h/R_0)^2}{\sqrt{1-\nu^2}} \qquad [3]$$

where the use of the outside radius R_0 is dictated by simple load equilibrium. In developing Equation [3] as a design equation, a sphere was considered near-perfect when its departures from sphericity over a critical length as defined in Reference 7, were less than 2 1/2 percent of a shell thickness. If small variations in shell thickness are present, the minimum shell thickness h_m should be substituted for h in Equation [3].

Tests have recently been conducted on machined deep spherical shells with known flat spots and thin spots.[8] To calculate the collapse strength of these initially imperfect spherical shells requires a close examination of the local imperfections. A preliminary evaluation of these test results, together with results of machined spherical segments with clamped boundaries[7] indicates that the elastic buckling strength of initially imperfect spherical shells is essentially a function of the local curvature and thickness of a segment of critical arc lengt L_c. This critical length is approximated by

$$L_c = \frac{2.2\,(R_1\,h_a)^{1/2}}{[3/4\,(1-\nu^2)]^{1/4}} \qquad [4]$$

The notation used for the imperfect shell is shown in Figure 2.

Thus, the elastic buckling pressure of an initially imperfect spherical shell may be estimated by using the following formula:[8]

$$P_3' = \frac{0.8E}{\sqrt{1-\nu^2}}\left(\frac{h_a}{R_{1_0}}\right)^2 \qquad [5]$$

Recent tests have also been conducted on hemispherical shells with varying boundary conditions.[9] These results have not been completely evaluated. However, test results of shells with rigid boundaries indicate that clamping the edge of a hemisphere may cause it to collapse elastically at a pressure about 10 to 20 percent below the collapse pressure of a complete sphere of the same thickness-to-radius ratio and the same magnitude of initial imperfections.

DESCRIPTION OF MODELS

Two series of ten hemispherical models of annealed Pyrex-brand borosilicate glass were procured. Pyrex-brand glass, which is designed by Corning Glass Works as No. 7740, has a Young's modulus E in the annealed condition of 9.07×10^6 psi, a Poisson's ratio of 0.19, and a specific gravity of 2.23.[9] One series of models, designated Models A through J, was manufactured by the National Bureau of Standards. These models were obtained by

parting a hand-blown spherical shell to provide an approximate 150-deg segment and by hand lapping the parted surface on a glass plate. The second series of models, manufactured by the Fisher and Porter Company and designated Models 1 through 10, was obtained by grinding and polishing a molded shell on all surfaces.

The wall thickness and local outside radii were measured for each model at predetermined orientations. In addition, the minimum shell thickness was also measured and recorded with respect to its angular orientation. The wall thickness of the hand-blown models was measured using a micrometer; the thickness of the ground and polished models was measured using a support and a dial gage calibrated in 0.0001 in. The local outside radii were measured in an identical manner for each model. The radii away from the edges were obtained by use of a dial gage supported by a hollow cylinder with an inside diameter of 0.53 in. First, the hollow cylinder with the attached dial gage was placed on a solid sphere of known radius and a reference reading was recorded. Then the support cylinder was placed on the spherical glass surface and dial readings were recorded at various orientations. By geometrically relating the dial reading obtained from the reference sphere to those obtained at various orientations on the glass hemispheres, the local outside radius R_L over 0.53-in. chord lengths was obtained. The local outside radius of the edges of the hemispheres was assumed to be equal to one-half the measured diameter. Photographs of these inspection procedures are shown in Figure 3. The measured wall thicknesses at various orientations are listed for the two series in Tables 1 and 2; the minimum measured wall thicknesses, the measured local outside radii at the point of minimum thickness, and other significant model dimensions are given in Table 3.

The calculated local outside radius over a 0.53-in. chord length varied considerably for the hand-blown models although in no instance did the variation occur abruptly. The calculated outside radius of the ground and polished models was, for all practical purposes, constant for each model. Thus, the variation in thickness for the ground and polished models was evidently a result of local variations in the inside radius and the improper location of the inside radius with respect to the outside radius.

TEST PROCEDURE AND RESULTS

Each model was sealed by placing PRC sealing compound between the glass and a heavy steel end plate and then subjected to external hydrostatic pressure in the 3-in., 50,000-psi pressure tank. Pressure was applied in increments during each test. Each new pressure was held at least 1 min, and the final pressure increment was less than 5 percent of the maximum pressure applied. Model 9 was removed from the tank and inspected after being subjected to a pressure of 38,500 psi. No damage or leakage was observed and, therefore, Model 9 was placed back into the tank and tested to collapse. No visual inspection of any other model was made during the tests.

The experimental collapse pressures are presented in Table 4. Collapse of each model occurred in a sudden, unmistakable fashion and left a completely crystallized residue. Figure 4 shows a typical model before and after test. Some of the models collapsed while pressure was being applied and others collapsed while the pressure load was being held constant. In no case was a "fall-off" in pressure observed prior to collapse.

DISCUSSION

Since all models had variations in thickness and initial departure from midsurface sphericity, their collapse strength can best be calculated using the empirical Equation [5]. Figure 5 presents a comparison of the experimental collapse pressures with the pressures calculated using Equation [5]. A summary of the measured and calculated geometry of the local imperfection, which was assumed to center about the point of minimum measured thickness, is given in Table 5. The measured local outside radius R_L is assumed to be equal to R_{1_0} for the hand-blown models since the average shell thickness over a critical length was not significantly greater than the minimum measured thickness. In addition, it could not be determined from the limited data recorded whether the local reduction in thickness occurred at the inner surface, at the outer surface, or at both surfaces.

The agreement between experimental collapse pressures and the pressures calculated using empirical Equation [5] was fairly good for most models. In general, the models which had thin spots near the edge of the hemisphere in contact with the steel closure plate (Models C, E, F, G, H, and J) all collapsed at pressures below those calculated using Formula [5]. This would be expected since previous tests have demonstrated that a rigid boundary lowers the elastic buckling strength of hemispherical shells.[9] All other models except Model 8 collapsed at pressures close to or in excess of the pressures calculated using Equation [5]. Although almost all models had considerable variation in thickness, and thus would be considered imperfect; many of the models had practically constant radii and thickness over a critical length. In addition, all models had extremely smooth surfaces. Thus, it is not surprising that several of the models collapsed at pressures approaching the classical buckling pressure for perfect spheres when based on local geometry over a critical length; i.e., some collapse pressures approach values 1.43 times the pressures calculated using Equation [5]. These tests once again support the validity of the classical small deflection buckling theory for perfect spheres. As in the case of machined metalic shells,[4] however, it does not appear that spherical shells can be manufactured or measured to the accuracy required to rely on the classical equation for design purposes.

The average calculated stresses at collapse in Models 9 and 10, based on local imperfection geometry, were almost 300,000 psi. Model 9 withstood stress levels of almost 300,000 psi without any visible cracking or permanent set. Since the collapse of Models 9 and 10 as well as all other models was apparently elastic (see Figure 5), these tests do not demonstrate the maximum strength of No. 7740 glass. However, it appears safe to conclude on

the basis of these tests that annealed No. 7740 glass has a compressive strength in excess of 300,000 psi. In fact, these tests certainly do not cast any doubt on the validity of Bridgman's work in which he obtained stresses of 800,000 psi in glass without causing any permanent deformation.[1] For practical deep-submergence applications, therefore, certain glass may be assumed to have an infinite compressive strength.

The strength-weight characteristics of these models are shown in Figure 6. The experimental points in Figure 6a are based on local geometry and thus represent weight-to-displacement ratios for essentially near-perfect spheres. The experimental data in Figure 6b are based on average measured thickness over the entire model and on nominal outside radius. Figure 6 demonstrates that the strength-weight characteristics of spherical glass shells, as well as of any other type of spherical shell, have little meaning unless local geometry is adequately defined. Figure 6 also demonstrates the influential role which manufacturing tolerances play on strength-weight characteristics, or structural efficiency, of spherical glass shells.

The estimated collapse depth versus ratio of weight to displacement for near-perfect spheres of various available materials is presented in Figure 7. The Model Basin empirical design equation was used in all calculations. Since many of the materials have nonlinear stress-strain characteristics, the general form of Equation [3], which accounts for reductions in secant and tangent modulus, was used.[3, 7, 8] Typical stress-strain curves were assumed in all calculations. It is apparent from Figure 7 that glass shows an outstanding strength-weight advantage over such materials as high-strength steels, glass-reinforced plastics, and aluminum and titanium alloys. For example, a No. 7740 glass sphere with a weight-displacement ratio of 0.4 has a static collapse depth approximately 10 times that of an HY-80 steel sphere of the same ratio. Pyroceram[10] spheres show promise of providing even higher strength-weight characteristics than do No. 7740 glass spheres.

Although No. 7740 glass and Pyroceram are the only two glassy materials shown in Figure 7, there are many more materials of this general type which give promise of yielding equal or even superior results. This fact has been emphasized by H.A. Perry of the Naval Ordnance Laboratory in a paper presented at the recent David Taylor Model Basin Workshop on Deep-Submergence Hulls. Perry has given this class of materials the name "bridgmanites" which he defines as follows:

> "A class of synthetic solids with minimum yield strength of at least one million psi and no creep at ordinary temperature. These solids are inorganic and amorphous, but may contain crystallites as a minor phase. The major phase may be a macromolecule. The bridgmanites include silica, the high-silicate glasses and glassy boron. The unique behavior of the high-silicate glasses under high pressure was first recognized by the late Professor P.W. Bridgman in whose memory this class of solids is named."

Based on the phenomenal strength-weight characteristics of bridgmanite structures as demonstrated in Figure 7, further investigation of the potential of such hulls for deep-submergence applications appears worthy. These possible applications range from glass

microballoons embedded in a plastic matrix, as currently being studied by numerous investigators, to hulls for manned vehicles ranging in diameter from about 6 to 30 ft. The tests reported herein have shown that on the basis of short-term static strength, the strength-to-weight characteristics of bridgmanites are far superior to those of other materials presently considered for deep-submergence applications. However, the long-term mechanical properties of bridgmanites in a marine environment have not been demonstrated. These critical properties include tensile strength, crack resistance, static fatigue (stress corrosion), cyclic fatigue, impact resistance, and creep. Until these material properties are determined under in-service conditions for economically feasible structural elements, the potential of these materials for deep-submergence applications cannot be properly assessed.

SUMMARY

1. The experimental collapse pressures were adequately calculated using empirical design Equation [5].

2. By obtaining isolated collapse pressures considerably above those calculated using Equation [5], these tests support the validity of the classical small deflection theory for initially perfect spheres.

3. Maximum stress levels of about 300,000 psi were obtained in these tests. However, these results do not demonstrate the maximum compressive strength of No. 7740 glass since each failure initiated in the elastic buckling range.

4. Manufacturing tolerances have a significant effect on the strength-to-weight characteristics of spherical glass shells.

5. Spheres composed of No. 7740 glass and other bridgmanite material have an outstanding strength-to-weight advantage over any other type hull using known materials. For example, a No. 7740 glass sphere with a weight-to-displacement ratio of 0.4 has about a 10 to 1 hydrostatic strength advantage over an HY-80 steel sphere of the same weight.

6. The long-term mechanical properties of bridgmanites in a marine environment must be evaluated before the potential of these materials for deep-submergence applications may be properly assessed.

RECOMMENDATIONS

1. Long-term mechanical properties of bridgmanites (such as tensile strength, crack resistance, static fatigue, cyclic fatigue, impact resistance, and creep) in a marine environment should be investigated.

2. A comprehensive investigation should be conducted of the potentials of bridgmanites as structural members or components of naval vessels and weapons and the problems involved in their use.

ACKNOWLEDGMENTS

The authors wish to express their appreciation to Mr. H. DeLeoniibus of the National Bureau of Standards who manufactured the hand-blown specimens and to Mr. L.J. Guiffredia who conducted the hydrostatic tests. The authors also wish to thank Mr. E.E. Johnson, Head, Ship Structures Division, and Mr. A.B. Stavovy, Head, Design Analysis Branch, for their continued interest in this project.

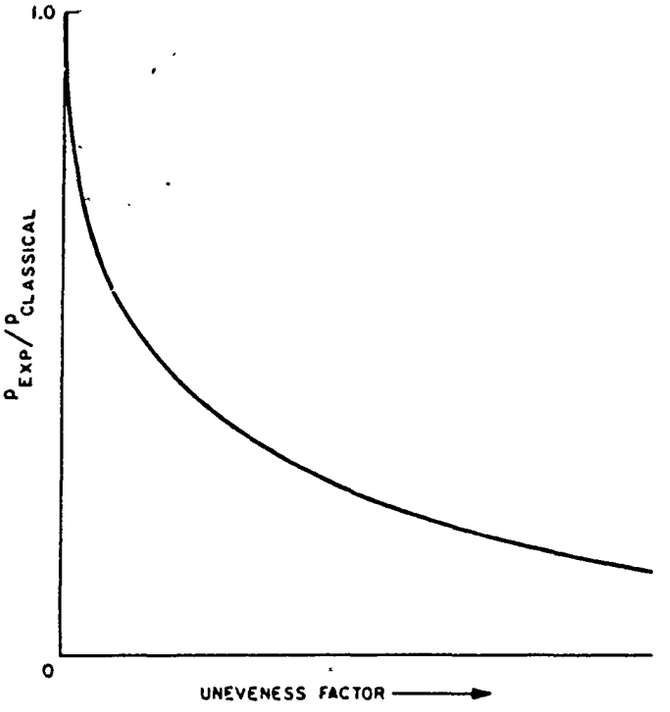

Figure 1 – Effect of Initial Imperfections on the Elastic Buckling Coefficient for Spherical Shells

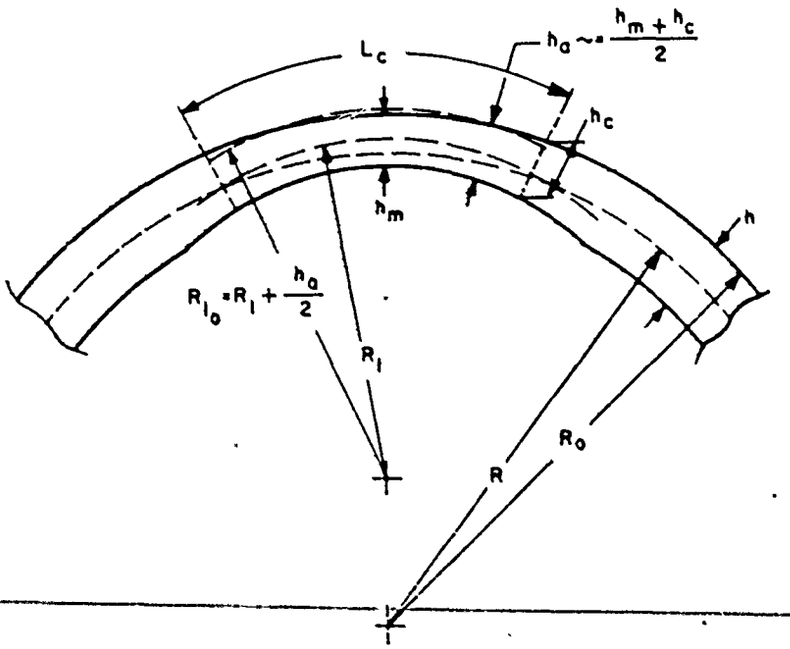

Figure 2 – Notation Used for the Imperfect Shell

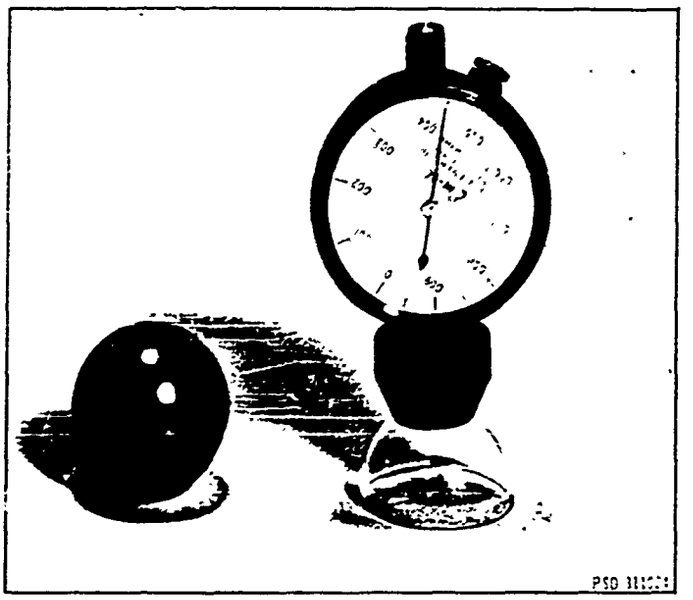

Figure 3a – Measuring Local Outside Radius

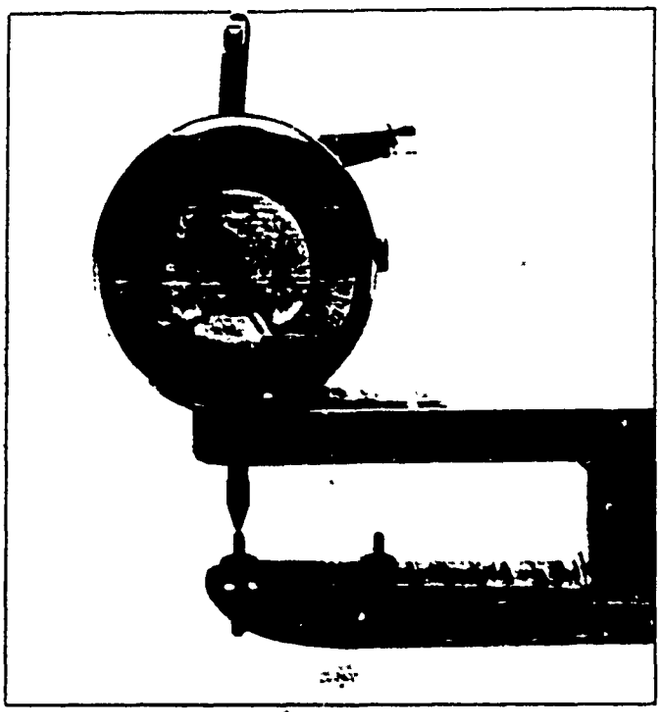

Figure 3b – Measuring Wall Thickness

Figure 3 – Model during Inspection

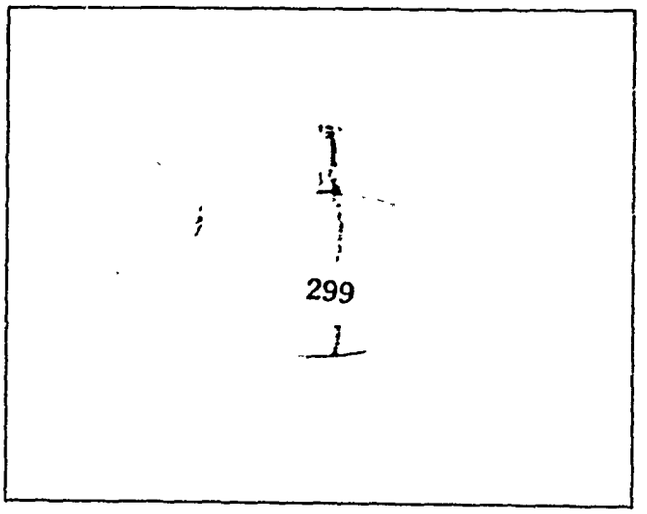

Figure 4a – Before Test

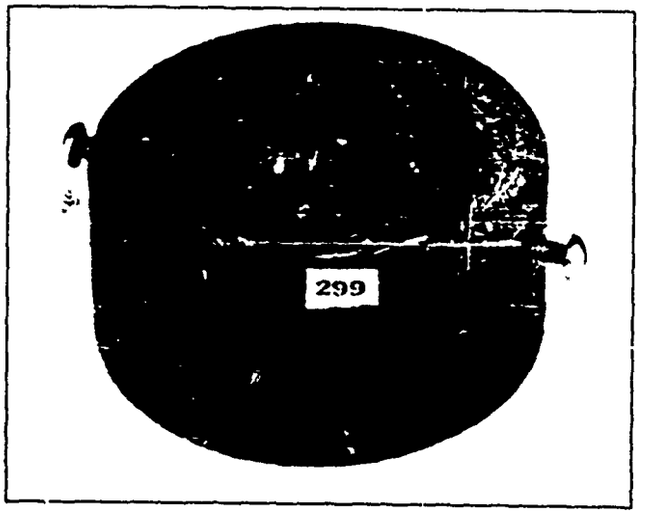

Figure 4b – After Test

Figure 4 – Model before and after Test

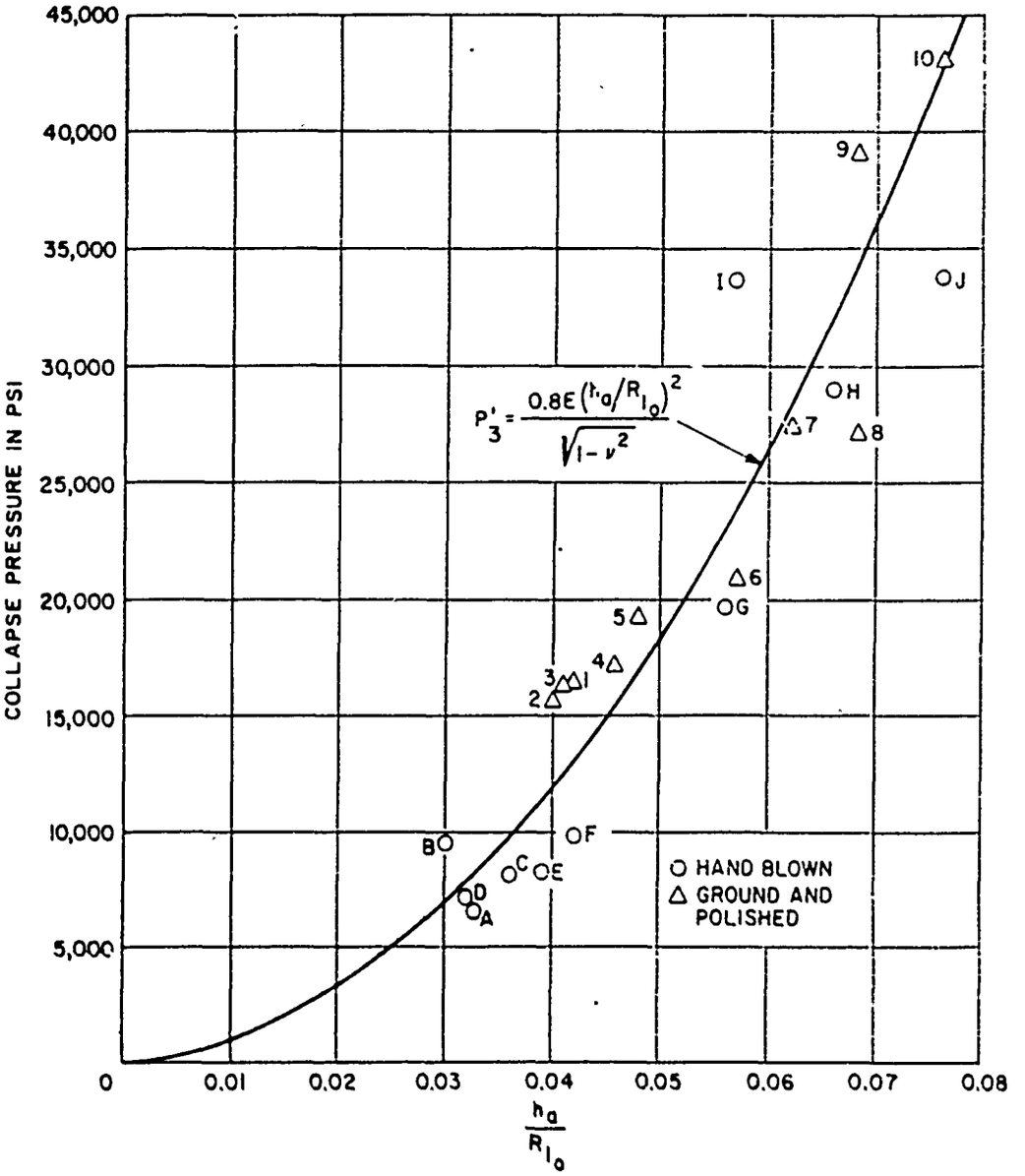

Figure 5 – Comparison of Experimental Collapse Pressure with Empirical Design Equation for Initially Imperfect Spheres

Figure 6 – Experimental Collapse Depth versus Ratio of Weight to Displacement

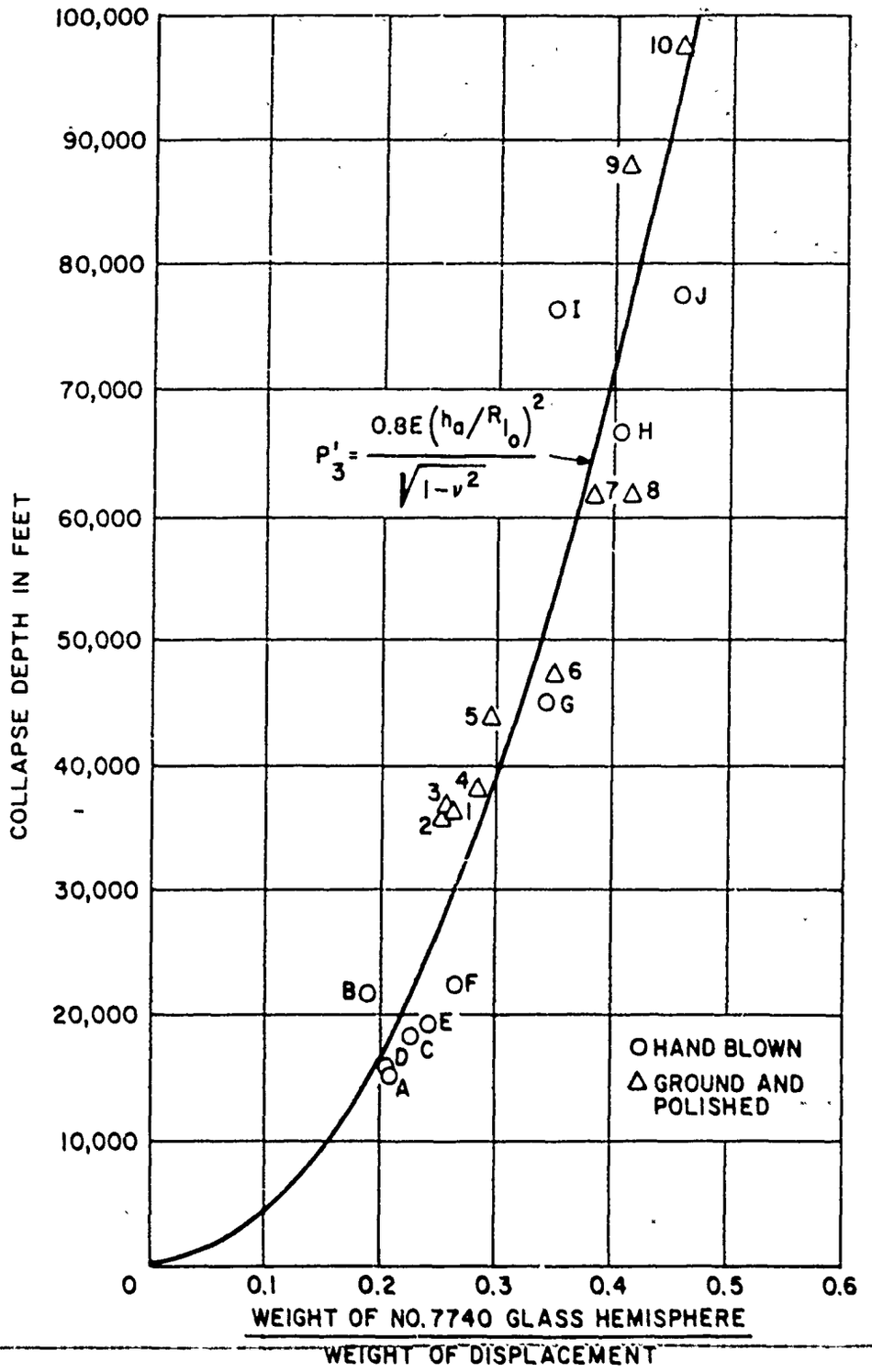

Figure 6a – Based on Local Imperfection Geometry

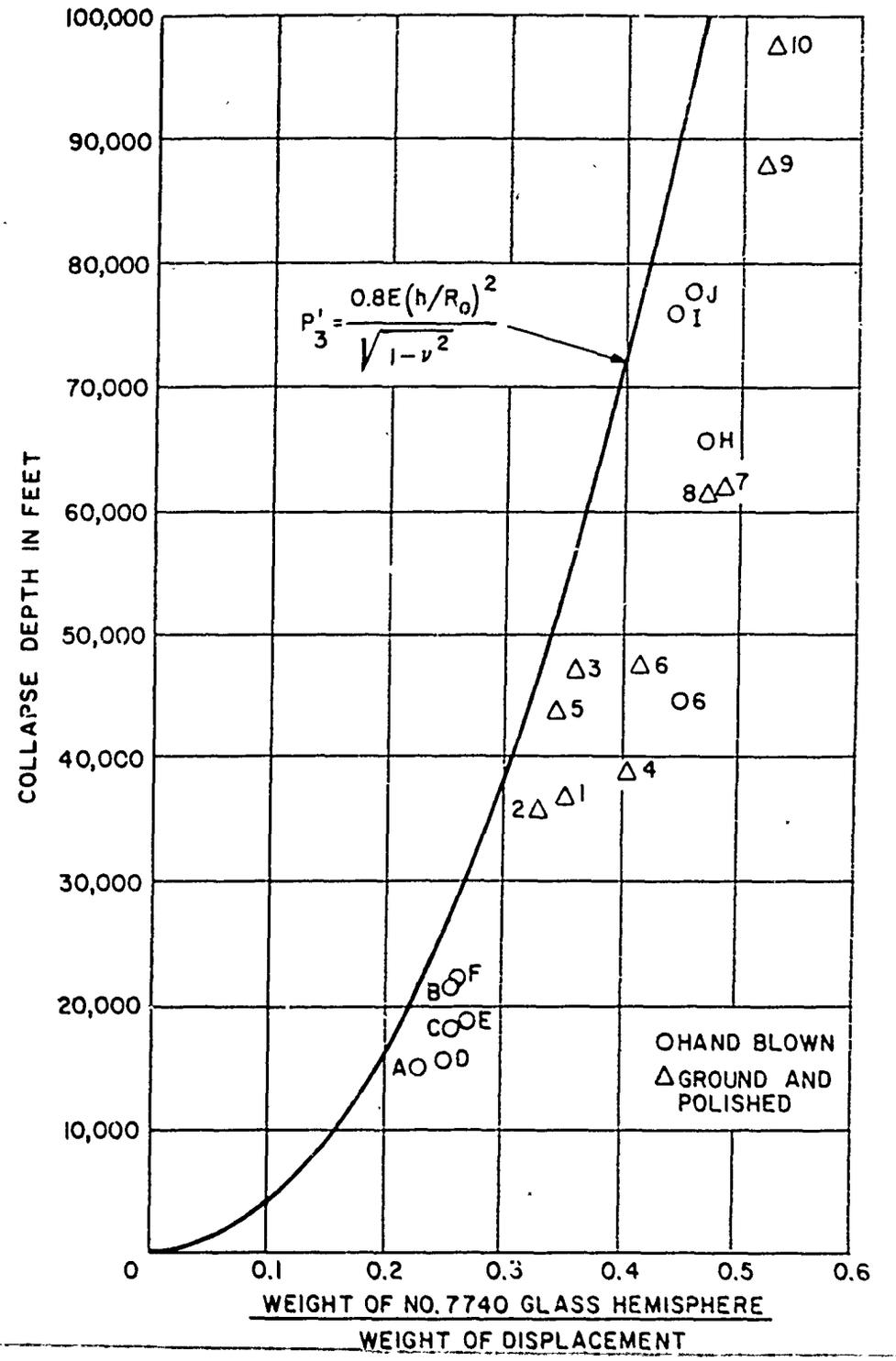

Figure 6b — Based on Nominal Geometry

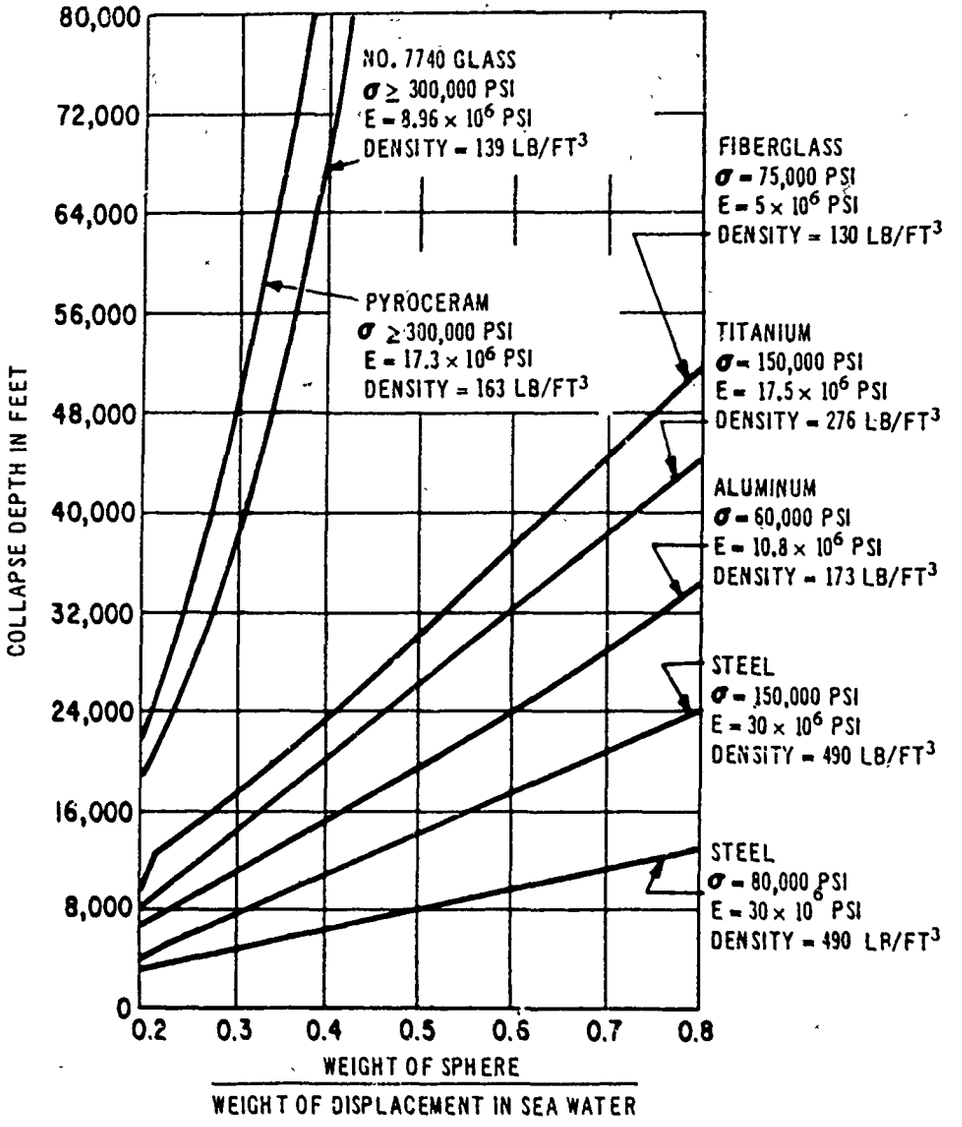

Figure 7 – Estimated Collapse Depth versus Ratio of Weight to Displacement for Near Perfect Spheres

TABLE 1

Measured Shell Thicknesses, Hand-Blown Series

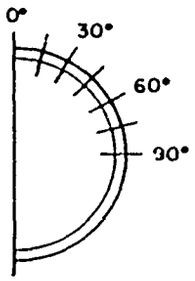

VERTICAL ORIENTATION

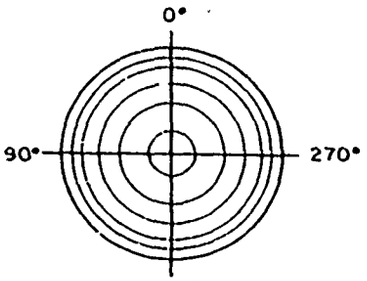

CIRCUMFERENTIAL ORIENTATION

Model	Circumferential Orientation deg	Measured Shell Thickness, in.															
		Vertical Orientation, deg													Minimum Thickness in.	Orientation of Minimum Thickness, deg	
		0	15	30	45	60	75	90	75	60	45	30	15	0		Circumferential	Vertical
A	0–180	0.028	0.027	0.026	0.027	0.027	0.030	0.031	0.027	0.026	0.025	0.026	0.028	0.029	0.025	270	45
	90–270	0.028	0.027	0.026	0.027	0.027	0.028	0.031	0.028	0.026	0.025	0.026	0.026	0.029			
B	0–180	0.035	0.034	0.032	0.028	0.026	0.026	0.030	0.027	0.029	0.029	0.032	0.033	0.033	0.025	60	75
	90–270	0.031	0.031	0.029	0.027	0.026	0.026	0.030	0.028	0.029	0.032	0.035	0.036	0.036			
C	0–180	0.027	0.028	0.028	0.029	0.032	0.032	0.033	0.032	0.033	0.033	0.032	0.031	0.029	0.026	270	0
	90–270	0.030	0.030	0.032	0.032	0.032	0.032	0.033	0.032	0.031	0.029	0.028	0.026	0.026			
D	0–180	0.030	0.028	0.028	0.029	0.029	0.031	0.033	0.030	0.028	0.027	0.029	0.031	0.032	0.027	180	45
	90–270	0.032	0.030	0.028	0.028	0.027	0.034	0.033	0.031	0.029	0.028	0.029	0.031	0.032			
E	0–180	0.030	0.030	0.030	0.030	0.032	0.032	0.034	0.033	0.031	0.031	0.033	0.031	0.032	0.029	345	5
	90–270	0.034	0.033	0.033	0.032	0.032	0.032	0.034	0.032	0.031	0.031	0.032	0.031	0.032			
F	0–180	0.032	0.033	0.037	0.043	0.050	0.054	0.061	0.056	0.050	0.047	0.039	0.035	0.035	0.032	0	0
	90–270	0.035	0.035	0.039	0.043	0.051	0.056	0.061	0.056	0.050	0.043	0.040	0.037	0.037			
G	0–180	0.041	0.044	0.050	0.059	0.061	0.062	0.065	0.068	0.068	0.059	0.054	0.046	0.046	0.041	0	0
	90–270	0.043	0.043	0.048	0.056	0.060	0.061	0.065	0.067	0.069	0.064	0.058	0.051	0.050			
H	0–180	0.050	0.051	0.054	0.055	0.055	0.058	0.065	0.063	0.063	0.064	0.065	0.058	0.055	0.049	45	0
	90–270	0.050	0.052	0.058	0.056	0.057	0.058	0.065	0.068	0.065	0.063	0.062	0.058	0.055			
I	0–180	0.055	0.054	0.055	0.055	0.056	0.059	0.060	0.056	0.055	0.053	0.052	0.050	0.049	0.048	90	45
	90–270	0.048	0.048	0.049	0.051	0.052	0.056	0.060	0.060	0.059	0.060	0.058	0.059	0.058			
J	0–180	0.058	0.061	0.070	0.080	0.083	0.083	0.082	0.087	0.081	0.078	0.071	0.060	0.056	0.056	90	0
	90–270	0.056	0.059	0.071	0.080	0.084	0.083	0.082	0.085	0.081	0.080	0.078	0.060	0.057			

TABLE 2

Measured Shell Thicknesses, Ground and Polished Series

Model	Circumferential Orientation deg	Measured Shell Thickness, in.									Minimum Thickness in.	Orientation of Minimum Thickness, deg	
		Vertical Orientation, deg										Circumferential	Vertical
		0	22.5	45	67.5	90	67.5	45	22.5	0			
1	0–180	0.0414	0.0321	0.0258	0.0245	0.0253	0.0245	0.0250	0.0308	0.0438	0.0201	90	55
	90–270	0.0373	0.0273	0.0224	0.0229	0.0253	0.0271	0.0315	0.0383	0.0479			
2	0–180	0.0371	0.0255	0.0234	0.0220	0.0217	0.0235	0.0258	0.0298	0.0375	0.0205	295	55
	90–270	0.0375	0.0304	0.0230	0.0255	0.0217	0.0211	0.0230	0.0306	0.0394			
3	0–180	0.0484	0.0325	0.0241	0.0225	0.0227	0.0241	0.0272	0.0345	0.0471	0.0223	23	70
	90–270	0.0439	0.0311	0.0248	0.0233	0.0227	0.0240	0.0266	0.0357	0.0507			
4	0–180	0.0504	0.0428	0.0309	0.0258	0.0264	0.0260	0.0325	0.0435	0.0513	0.0246	295	55
	90–270	0.0508	0.0448	0.0341	0.0276	0.0264	0.0248	0.0279	0.0384	0.0500			
5	0–180	0.0529	0.0334	0.0271	0.0261	0.0291	0.0265	0.0298	0.0395	0.0595	0.0256	22	60
	90–270	0.0556	0.0361	0.0289	0.0253	0.0291	0.0272	0.0294	0.0370	0.0555			
6	0–180	0.0515	0.0393	0.0317	0.0310	0.0322	0.0314	0.0318	0.0364	0.0488	0.0305	225	55
	90–270	0.0495	0.0366	0.0322	0.0316	0.0322	0.0314	0.0321	0.0375	0.0502			
7	0–180	0.0531	0.0417	0.0367	0.0368	0.0360	0.0350	0.0380	0.0448	0.0609	0.0345	295	60
	90–270	0.0549	0.0422	0.0371	0.0356	0.0360	0.0347	0.0359	0.0432	0.0569			
8	0–180	0.0500	0.0488	0.0425	0.0387	0.0401	0.0365	0.0365	0.0428	0.0531	0.0355	155	55
	90–270	0.0551	0.0442	0.0380	0.0372	0.0401	0.0377	0.0393	0.0460	0.0570			
9	0–180	0.0567	0.0442	0.0394	0.0390	0.0400	0.0394	0.0416	0.0470	0.0631	0.0390	0	55
	90–270	0.0620	0.0444	0.0400	0.0386	0.0400	0.0390	0.0411	0.0464	0.0530			
10	0–180	0.0533	0.0479	0.0421	0.0421	0.0411	0.0429	0.0430	0.0498	0.0546	0.0408	110	50
	90–270	0.0539	0.0472	0.0416	0.0415	0.0411	0.0430	0.0432	0.0483	0.0537			

TABLE 3

Measured Model Dimensions

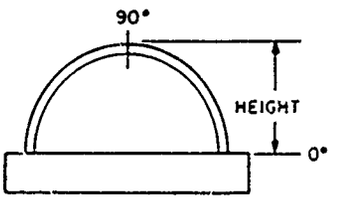

Series	Model	Average Thickness in.	Maximum Thickness in.	Minimum Thickness in.	Vertical Angle Location of Minimum Thickness deg	Nominal Outside Radius in.	Local Outside Radius at Minimum Thickness in.	Height in.
Hand Blown	A	0.0272	0.031	0.025	45	0.75	0.753	0.757
	B	0.0304	0.036	0.025	75	0.75	0.825	0.793
	C	0.0304	0.033	0.026	0	0.75	0.751	0.725
	D	0.0298	0.034	0.027	45	0.75	0.832*	0.793
	E	0.0318	0.034	0.029	5	0.75	0.751	0.803
	F	0.0438	0.067	0.032	0	0.75	0.757	0.801
	G	0.0557	0.069	0.041	0	0.75	0.755	0.736
	H	0.0583	0.068	0.049	0	0.75	0.753	0.724
	I	0.0547	0.060	0.048	45	0.75	0.847	0.730
	J	0.073	0.087	0.056	0	0.75	0.750	0.745
Ground and Polished	1	0.0312	0.0479	0.0201	55	0.55	0.555	0.504
	2	0.0284	0.0394	0.0205	65	0.54	0.550	0.521
	3	0.0319	0.0507	0.0223	70	0.55	0.567	0.499
	4	0.0369	0.0513	0.0246	65	0.56	0.570	0.499
	5	0.0365	0.0595	0.0256	60	0.56	0.567	0.527
	6	0.0374	0.0515	0.0305	55	0.55	0.560	0.541
	7	0.0425	0.0569	0.0345	60	0.56	0.580	0.523
	8	0.0443	0.060	0.0355	55	0.57	0.570	0.525
	9	0.0458	0.0631	0.0330	65	0.56	0.570	0.522
	10	0.0464	0.0546	0.0408	60	0.56	0.570	0.537

*Estimated

TABLE 4

Experimental Collapse Pressures

Series	Model	Experimental Collapse Pressure psi
Hand Blown	A	6,700
	B	9,500
	C	8,150
	D	7,000
	E	8,400
	F	9,850
	G	13,800
	H	29,000
	I	33,750
	J	34,500
Ground and Polished	1	16,250
	2	15,850
	3	16,450
	4	17,250
	5	19,450
	6	21,000
	7	27,500
	8	27,250
	9	39,000
	10	43,250

TABLE 5

Critical Imperfection Geometry

Series	Model	λ_m, in.	λ_c, in.	λ_a, in.	$\frac{R_1}{R}$	R_{1_0}, in.
Hand Blown	A	0.025	0.026	0.025	~1.00	0.753
	B	0.025	0.026	0.025		0.825
	C	0.026	0.028	0.027		0.751
	D	0.027	0.028	0.027		0.832
	E	0.029	0.030	0.029		0.751
	F	0.032	0.033	0.032		0.757
	G	0.041	0.043	0.042		0.755
	H	0.049	0.051	0.050		0.753
	I	0.048	0.049	0.048		0.847
	J	0.056	0.058	0.057		0.750
Ground and Polished	1	0.0201	0.023	0.021	0.90	0.501
	2	0.0205	0.022	0.021	0.95	0.523
	3	0.0223	0.023	0.023	0.98	0.556
	4	0.0246	0.026	0.025	0.96	0.548
	5	0.0256	0.027	0.026	0.96	0.545
	6	0.0305	0.032	0.031	0.97	0.544
	7	0.0345	0.036	0.035	0.97	0.563
	8	0.0355	0.038	0.037	0.95	0.542
	9	0.0380	0.039	0.038	0.98	0.559
	10	0.0403	0.043	0.042	0.97	0.554

REFERENCES

1. Bridgman, P.W., "Studies in Large Plastic Flow and Fracture (with Special Emphasis on the Effects of Hydrostatic Pressure)," McGraw-Hill Book Company, Inc., New York (1952).

2. Krenzko, M.A., "Exploratory Tests of Long Glass Cylinders under External Hydrostatic Pressure," David Taylor Model Basin Report 1641 (Aug 1962).

3. Krenzke, M.A., "Tests of Machined Deep Spherical Shells under External Hydrostatic Pressure," David Taylor Model Basin Report 1601 (May 1962).

4. Krenzke, M.A., "The Elastic Buckling Strength of Near-Perfect Deep Spherical Shells with Ideal Boundaries," David Taylor Model Basin Report 1713 (July 1963).

5. Timoshenko, S., "Theory of Elastic Stability," McGraw-Hill Book Co., Inc., New York (1936).

6. Fung, V.C. and Seckler, E.E., "Instability of Thin Elastic Shell," Proceedings of the First Symposium on Naval Structural Mechanics (1960).

7. Krenzke, M.A. and Kiernan, T.J., "Tests of Stiffened and Unstiffened Machined Spherical Shells under External Hydrostatic Pressure," David Taylor Model Basin Report 1741 (Aug 1963).

8. Krenzke, M.A. and Kiernan, T.J., "The Effect of Initial Imperfections on the Collapse Strength of Deep Spherical Shells," David Taylor Model Basin Report 1757 (in preparation).

9. Kiernan, T.J., "The Effects of Boundary Conditions on the Collapse Strength of Machined Hemispherical Shells under External Hydrostatic Pressure," David Taylor Model Basin Report (in preparation).

10. Kerper, M.J., et al., "Properties of Glass at Elevated Temperatures," Wright Air Development Center Report 56-645, Part III (Dec 1958).

INITIAL DISTRIBUTION

Copies	
18	CHBUSHIPS
	2 Sci & Res Sec (Code 442)
	3 Tech Lib (Code 210L)
	1 Lab Mgt (Code 320)
	2 Struc Mech, Hull Mat & Fab (Code 341A)
	1 Prelim Des Br (Code 420)
	1 Prelim Des Sec (Code 421)
	1 Ship Protec (Code 423)
	1 Hull Des (Code 440)
	1 Hull Struc (Code 443)
	2 Sub Br (Code 525)
	2 Polymer, Fiber Packaging Sec (Code 634C)
	1 Pres Ves (Code 651F)
3	CHONR
	1 Struc Mech (Code 439)
	2 U/Sea Programs (Code 466)
4	CNO
	1 (Op 311)
	1 (Op 07T)
	1 (Op 713)
	1 (Op 725)
10	CDR, DDC
1	CO & DIR, USNMEL
1	CDR, USNOL
1	DIR, USNRL (2027)
1	CO & DIR, USNUSL
1	CO & DIR, USNEL
1	CDR, USNOTS, China Lake
1	CDR, USNOTS, Pasadena
1	CO, USNUOS
1	NASL
2	NAVSHIPYD PTSMH
2	NAVSHIPYD MARE
1	NAVSHIPYD CHASN
1	SUPSHIP, Groton
1	EB Div, Gen Dyn Corp
1	SUPSHIP, Newport News

Copies	
1	NNSB & DD Co
1	SUPSHIP, Pascagoula
1	Ingalls Shipbldg Corp
1	SUPSHIP, Camden
1	New York Shipbldg
1	DIR, DEF R & E, Attn: Tech Lib
1	CO, USNROTC & NAVADMINU, MIT
1	O in C, PGSCOL, Webb
1	DIR, APL, Univ of Wash, Seattle
1	NAS, Attn: Comm on Undersea Warfare
1	Prof. J. Kempner, PIB
1	Dr. E. Wenk, Jr., The White House
1	Dr. R. DeHart, Southwest Res Inst
1	Mr. Leonard P. Zick, Chic Bridge & Iron Co.
1	Dean V.L. Salerno, Fairleigh Dickinson Univ
1	Prof. E.O. Waters, Yale Univ
2	Mr. C.F. Larson, Secretary, Welding Res Council
1	Prof. Bernard Budiansky, Harvard Univ